Analysis of a system of two masses linked by a rope with variable tension including a friction force

H. J. Herrera-Suárez
Semillero NOVAMAT, Facultad de Ciencias Naturales y Matemáticas, Universidad de Ibagué, Carrera 22 Calle 67, barrio Ambalá, Ibagué, 730002, Colombia

M. Machado-Higuera
Facultad de Ciencias Naturales y Matemáticas, Universidad de Ibagué, Carrera 22 Calle 67, barrio Ambalá, Ibagué, 730002, Colombia.

J. H. Muñoz
Universidad del Tolima, Departamento de Física, Código Postal 730006299, Ibagué-Colombia.

Received 13 August 2024; accepted 25 September 2024

The effect of a friction force on a system consisting of a two masses connected by a rope passing over a frictionless pulley is investigated. One mass slides on a horizontal surface with friction, while the other mass moves vertically. The motion equation is obtained and its numerical solution is computed using the `GNU Octave` package. The experimental data are obtained using a data acquisition system and the `Tracker` video analyser. The graphs are made using the `Origin` software. The vertical position of one of the masses in function of the time can be represented by an exponential expression of the form $y(t) = ab^t$. The comparison between theoretical and experimental results gives that the lowest average relative error is obtained with the `Tracker`.

Keywords: Newton's laws; mechanics; variable tension.

DOI: https://doi.org/10.31349/RevMexFisE.22.020206

1. Introduction

This study carries out an exhaustive analysis of a system composed of two masses, named m_1 and m_2, which are connected by a rope of constant length, moving on a frictionless pulley. As the mass m_2 descends, the mass m_1 moves on a horizontal plane, with a dynamic coefficient of friction $\mu_k = 0.31$. The rope connecting the masses is uniform, with no stretch and negligible mass. This configuration allows the system to experience a time-varying acceleration. In Fig. 1, the forces in this setup are shown, identifying f_f as the frictional force and g as the acceleration due to gravity.

In this system, the tension T, the normal force N, and the acceleration are not constant. It is a more complex problem than traditional systems conformed by two masses connected by a string that passes by a pulley with a constant tension (the so-called Atwood-type machine).

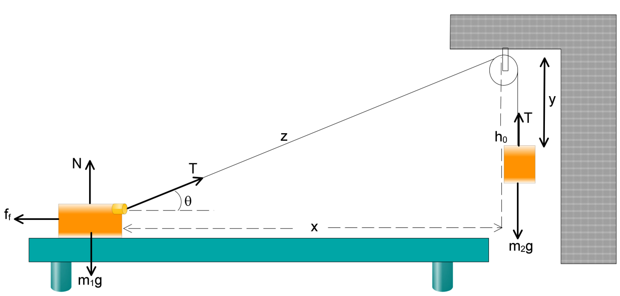

FIGURE 1. Two blocks connected by a non-stretchable rope. Mass m_2 descends vertically, while mass m_1 moves along the horizontal surface.

The static equilibrium of this system has been analyzed previously in the literature [1–13]. However, there are some important details, when performing a deep review, that have not been reported yet. On the other hand, the dynamic situation without friction has also been studied by some authors [1,2,14,15]. In this work, the dynamic case with friction between m_1 and the horizontal surface is investigated. The purpose is to scrutinize this system more, perform a complete analysis, and extend our previous works [12, 14].

At the theoretical level, the motion equation is explicitly obtained, and its numerical solution is achieved using the `GNU Octave` package [16]. At the experimental level, a similar montage presented in reference [14] is performed. The data for y vs t are taken using a data acquisition system (DAS) and the `Tracker` video analyser [17]. The graphs are implemented using the `Origin` software [18].

The problem analyzed in this paper allows the use of computational and technological tools and checks the experimental feasibility of some theoretical problems studied in some physics textbooks. These strategies have a pedagogical value and contribute to improving teaching practice. They promote an articulation between theory and experiment and furnish a better student's understanding of physics.

This paper is organized as follows: the theoretical analysis is shown in Sec. 2. The Sec. 3 presents the theoretical and experimental results obtained. The Sec. 4 contains the summary of our study.

2. Theoretical analysis

Applying Newton's second law on particle m_1 (see Fig. 1) in the x and y directions is obtained

$$T\cos\theta - \mu_k N = m_1 a_x, \tag{1}$$

$$T\sin\theta + N - m_1 g = 0. \tag{2}$$

From the Eq. (2), the normal force is

$$N = m_1 g - T\sin\theta. \tag{3}$$

Replacing this expression for N in Eq. (1), it is obtained

$$T\left(\cos\theta + \mu_k \sin\theta\right) - \mu_k m_1 g = m_1 a_x. \tag{4}$$

On the other hand, the sum of the forces acting on mass m_2 (see Fig. 1) in the y direction gives

$$T - m_2 g = -m_2 a_y. \tag{5}$$

The tension T is obtained from Eq. (5), and by substituting it in Eq. (4), it is obtained

$$(m_2 g - m_2 a_y)\left(\frac{x + \mu_k h_0}{\sqrt{x^2 + h_0^2}}\right) - \mu_k m_1 g = m_1 a_x, \tag{6}$$

where it was used that $\cos\theta = x/z = x/\sqrt{x^2 + h_0^2}$ and $\sin\theta = h_0/z = h_0/\sqrt{x^2 + h_0^2}$ (according to Fig. 1). On the other hand, the length l of the rope is given by $l = \sqrt{x^2 + h_0^2} + y$. From this expression, it is obtained $x^2 = (l - y)^2 - h_0^2$; deriving it gives the velocity in y

$$v_y = -x v_x (x^2 + h_0^2)^{-\frac{1}{2}}, \tag{7}$$

where $v_x = dx/dt$ and $v_y = dy/dt$ are the speeds of mass m_1 and m_2, respectively. Now, by differentiating Eq. (7) with respect to time, it is obtained the following expression

$$a_x = -\frac{h_0^2 v_y^2}{\left((l - y)^2 - h_0^2\right)^{\frac{3}{2}}} - \frac{(l - y)\, a_y}{\left((l - y)^2 - h_0^2\right)^{\frac{1}{2}}}, \tag{8}$$

in this context, $a_x = dv_x/dt$ and $a_y = dv_y/dt$ are the corresponding accelerations. Upon substituting the expression (8) into Eq. (6), we derive the subsequent expression:

$$a_y = \frac{m_2 g\,(x + \mu_k h_0)\, x^3 + m_1 v_y^2 h_0^2\,(l - y) - \mu_k m_1 g\,(l - y)\, x^3}{x^2\left(m_2\,(x^2 + \mu_k h_0 x) - m_1\,(l - y)^2\right)}, \tag{9}$$

noting that Eq. (9) represents the variable of acceleration. Now, we are going two consider to special cases:

First case: static situation

This configuration is obtained assuming $a_x = 0 = a_y$, $v_x = 0 = v_y$ and $\mu_k = \mu_s$ in Eq. (9). This substitution gives

$$m_2 g = \frac{\mu_s m_1 g}{(\cos\theta + \mu_s \sin\theta)}, \tag{10}$$

in this case $T = m_2 g$, thus:

$$T = \frac{\mu_s m_1 g}{(\cos\theta + \mu_s \sin\theta)}. \tag{11}$$

This expression agrees with the equation reported in the textbooks [1–6] and the articles [7–12], for the static situation. So, it is demonstrated that Eq. (9) reproduces the tension reported in these references.

Substituting Eq. (11) in Eq. (3), it is obtained the normal N in function of the angle θ:

$$N = \frac{m_1 g \cos\theta}{(\cos\theta + \mu_s \sin\theta)}. \tag{12}$$

On the other hand, comparing Eqs. (10) and (11) it is obtained: $m_2/m_1 = T/m_1 g$. Figure 2 shows $T/m_1 g$ versus θ (red solid dots) and $N/m_1 g$ versus θ (black solid dots). It can be seen that N decreases in $[0, \pi/2]$. When the tension and the normal are equal, the following is obtained

$$\frac{\mu_s m_1 g}{\cos\theta + \mu_s \sin\theta} = \frac{m_1 g \cos\theta}{\cos\theta + \mu_s \sin\theta},$$

canceling similar terms

$$\cos\theta = \mu_s,$$

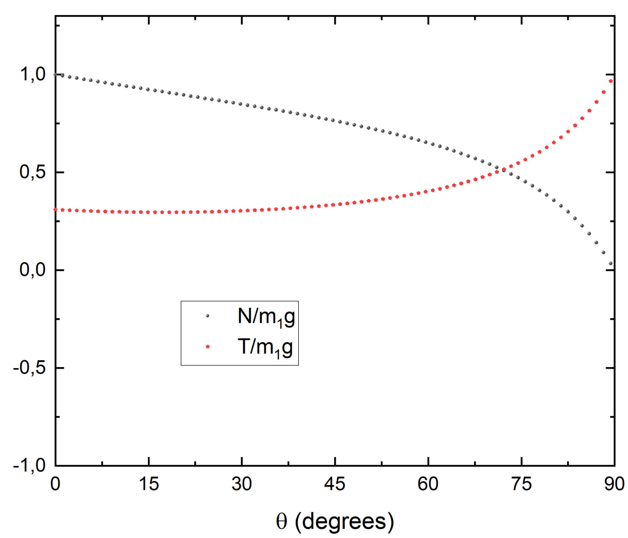

FIGURE 2. The red solid dots represent $T/m_1 g$ vs θ and the black dots show $N/m_1 g$ vs θ, with $\mu_s = 0.31$.

therefore

$$\theta = \cos^{-1}\mu_s. \tag{13}$$

It should be noted that the graphs in Fig. 2 are very different for small values of θ and μ_s

Second case: dynamic situation without friction

This configuration is obtained by assuming that $\mu_k = 0$. Replacing $\mu_k = 0$ in Eq. (9), the acceleration can be expressed as

$$a_y = \frac{m_2 g\left(\left(l-y\right)^2 - h_0^2\right)^2 + m_1 v_y^2 h_0^2\left(l-y\right)}{\left[\left(l-y\right)^2 - h_0^2\right]\left[m_2\left(\left(l-y\right)^2 - h_0^2\right) - m_1\left(l-y\right)^2\right]}. \tag{14}$$

This result agrees with the acceleration reported in the Eq. (8) of Ref. [14]. Thus, it is demonstrated that Eq. (9) reproduces the acceleration reported previously.

2.1. Numerical solution

The Eq. (9) is solved numerically using the `GNU Octave` package. First, it is defined the function with the differential equation. Secondly, the numerical solution is calculated with the command "**lsode**". And finally it is graphed.

The following commands in `GNU Octave` are essential to analyzing the system:

```
function Ydot = fcn(y,t)
m1=0.2829; m2=0.10;
L=2.03; h=0.52;
muk = 0.310; g=9.8;
% y1 = y (position)
% y2 = Vy (velocity)
b = m2 * g * ((sqrt((L - (y(1)))^2 - h^2)) + muk * h)... * (sqrt((L-(y(1)))^2-h^2))^3+m1*(h^2)...*((y(2))^2)*(L-y(1))-muk*m1*g*(L-y(1))*((sqrt((L-y(1))^2-h^2))^3);
a = ((L-((y(1))))^2-h^2)...*(m2*((L-y(1))^2-h^2+muk*h... * (sqrt((L - ((y(1))))^2 - h^2))) - m1 * ((L - y(1))^2))
Ydot(1) = y(2);
Ydot(2) = (b/a);
Ydot(1) = y(2);
Ydot(2) = (b/a);
endfunction
% inital conditions for solving
y0=[-0.088;-0.54];
t=[0:0.01:1]';
z=lsode(@Ydot,y0,t);
% Graph
figure(1)
plot (t, z(:,1),'r-', 'markersize', 5, 'linewidth', 1.7);
grid on;
xlabel("Time");
title("Pisition on y");
ylabel("y");
hold on
plot(t_DAS, -y_DAS,'b-','markersize', 5,
'linewidth', 1.5);
hold on
plot(t_Tracker, -y_Tracker,'k-','markersize', 5,
'linewidth', 1.5); legend('Octave','DAS','Tracker');
title("Position on 'y'")
```

3. Theoretical and experimental results

Figure 3 shows the experimental configuration when there is a friction force between m_1 and the horizontal surface. In this case, the air supply was not used. Table I shows the numerical parameters used in the experiment.

The data for the variable y in function of the time were registered with the `DAS` with the initial condition $y(0) = (-0.088 \pm 0.01)$ m. The movement of the two masses was also recorded with a smartphone, and this video was analyzed using `Tracker` video analyser [17]. The variation of y in function of the time t has been obtained using: (a) `Tracker` (b) `DAS` and (c) `GNU Octave` software.

Applying the same methodology used in Ref. [14], Fig. 4 shows the vertical movement of the mass m_2 using `Tracker`, `GNU Octave` and `DAS`. `Origin` software was used to make Fig. 4.

As mentioned before, Eq. (9) was solved with `GNU Octave` software, using the *lsode* function, to obtain the numerical solution of the differential equation. This solution is displayed in Fig. 4 (see the solid red circles). This figure shows

TABLE I. Numerical parameters used in the experiment.

Parameter	Value
Mass (m_1)	(0.2829 ± 0.01) kg [25]
Mass (m_2)	(0.10 ± 0.01) kg [25]
Chain length (l)	(2.03 ± 0.01) m
Initial height (h_0)	(0.52 ± 0.01) m
Gravity (g)	9.8 m/s^2
Coefficient kinetic friction (μ_k)	0.310

FIGURE 3. Experimental configuration: (a) computer; (b) combination spoked wheel [19]; (c) air track [20]; (d) sensor CASSY 2 [21] ; (e) timer S [22]; (f) multi-core cable, 6 poles, 1.5 m [23]; (g) combination light barrier [24]; (h) mass m_1, and (i) mass m_2.

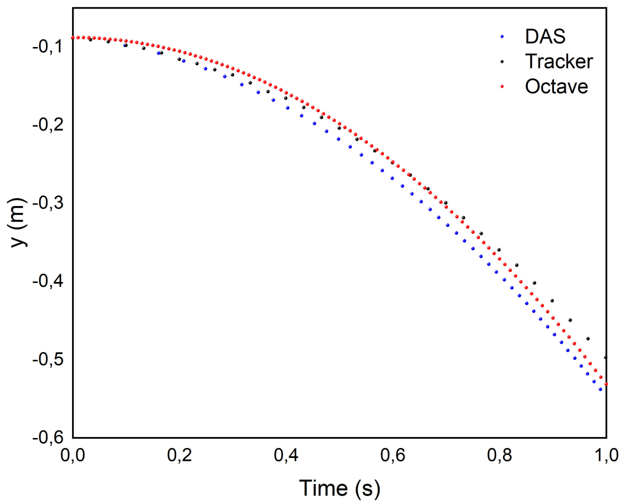

FIGURE 4. Displacement y of the mass m_2 as a function of time t.

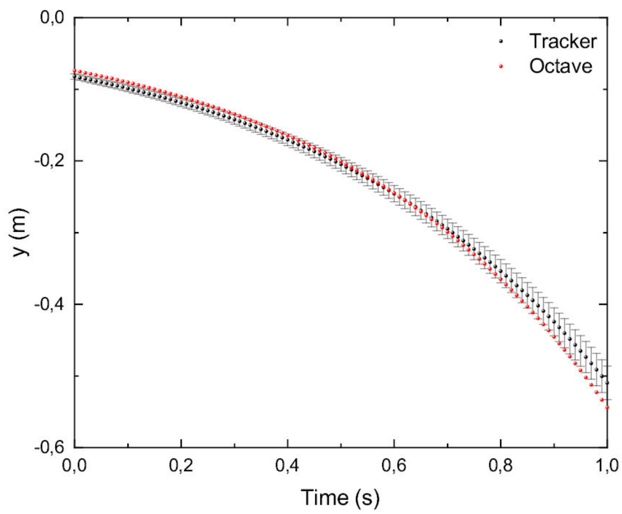

FIGURE 5. Results from `GNU Octave` and `Tracker`.

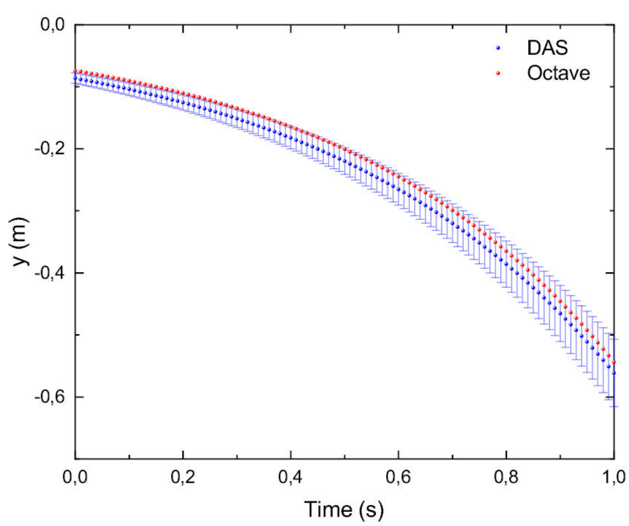

FIGURE 6. Results from `GNU Octave` and `DAS`.

TABLE II. y versus t for the data obtained using `GNU Octave`, the `DAS`, and `Tracker`.

Solution	Exponential adjustment
`GNU Octave`	$y(t) = -0.07396\,(7.35596)^t$
`DAS`	$y(t) = -0.08612\,(6.51952)^t$
`Tracker`	$y(t) = -0.08225\,(6.19513)^t$

that the motion of the mass m_2 registered by `Tracker` takes more time to travel the same distance when compared with the results obtained by `DAS`. The general configuration of the graph, together with the spatial arrangement of the data points, clearly suggests an exponential correlation between the y-variable and time.

Figures 5 and 6 show the comparison between the experimental data obtained using the Tracker and the `Data Acquisition System` (`DAS`) with the theoretical results derived from Octave, respectively.

In order to compare them, they were adjusted to exponential functions (see Table II) whose correlation coefficient was 0.998, obtaining an average relative error of 4.66% between the Tracker results and the theoretical approach. In addition, an average relative error of 9.68% was obtained when comparing the `DAS` results with the theoretical solution.

4. Summary

A general analysis of the system shown in Fig. I has been performed, considering the dynamic case with friction. The experimental analysis was carried out with two technological tools: (i) DAS and (ii) `Tracker`. The theoretical solution for the motion equation was obtained using `GNU Octave` software and the errors were calculated using `Origin`. Results previously reported in the literature for the static case [12] and for the dynamic case without friction [14] are reproduced.

When the friction between m_1 and the horizontal surface is considered, the movement of the mass m_2 along the y-axis is not uniformly accelerated. The integration of theoretical analysis, utilizing the `GNU Octave` software, with experimental data gathered through a `Data Acquisition System` (`DAS`) and `Tracker`, revealed an exponential correlation between the variable 'y' and time: $y = a * b^t$ (see Table II).

A comparative analysis between data acquired through `DAS` and Tracker video analysis with theoretical predictions from `GNU Octave` software indicated that the `Tracker` provided the most accurate results, with an average relative error of 4.66 %. This finding underscores the importance of selecting appropriate data acquisition methods for precise experimental physics.

This work is a continuation of previous works. It extends the knowledge of the system of two masses tied to a rope. The system studied in this work allows the articulation of theory and practice and the use of computational tools that help the understanding of physics.

1. R. A. Serway and J. W. Jewett, Physics for Scientists and Engineers with Modern Physics, 10th ed. (Cengage, Boston, 2019).
2. R. A. Serway and J. W. Jewett, Physics for Scientists and Engineers with Modern Physics Instructor Solutions Manual, 9th ed. (Cengage Learning, Boston, 2014)
3. F. A. González and M. Martínez Hernández, Problemas de física general, 1st ed. (Tebar Florez, España, 1978).
4. H. C. Ohanian and J. T. Markert, Physics for Engineers and Scientists, 3rd ed. (W. W. Norton & Company, NY, 2007).
5. R. C. Hibbeler, Engineering Mechanics - Dynamics, 15th ed. (Pearson, Reino Unido, 2022).
6. W. F. Riley, L. D. Sturges, Engineering Mechanics: Dynamics, 2nd ed. (John Wiley and Sons, Australia, 1996).
7. N. Lerman, Open-Ended Problem Instruction in General Physics, *Am. J. Phys.* **32** (1964) 927, `https://doi.org/10.1119/1.1970026`.
8. S. Mak, Extreme values problems in mechanics without calculus, *Am. J. Phys.* **55** (1987) 929, `https://doi.org/10.1119/1.14907`
9. D. Sütt, Elementary discussion of an optimization problem concerning friction, *Phys. Educ*. **29** (1994) 249, `https://iopscience.iop.org/article/10.1088/0031-9120/29/4/013`.
10. W. H. Van den Berg, The best angle for dragging a box, *Phys. Teach.* **38** (2000) 506, `https://doi.org/10.1119/1.1329099`.
11. W. J. Leonard, Dragging a Box: The representation of constraints and the constraint of representations, *Phys. Teach.* **39** (2001) 412, `https://doi.org/10.1119/1.1416311`.
12. D. Benitez, H. J. Herrera-Suárez and J. H. Muñoz, Symmetry in the System of Two Blocks Connected by a String with Variable Tension, *Rev. Cub. Phys.* **36** (2019) 139,
13. A. F. García, The best angle to drag a block, `http://www.sc.ehu.es/sbweb/fisica3/dinamica/arrastra/arrastra.html`
14. H. J. Herrera-Suárez, M. Machado-Higuera and J. H. Muñoz, *Phys. Educ.* **55** (2020) 055022, `https://dx.doi.org/10.1088/1361-6552/ab9956`
15. C. E. Mungan, Comment on ’Two blocks connected by a string with variable tension: a dynamic case’, *Phys. Educ.* **56** (2021) 028001, `https://dx.doi.org/10.1088/1361-6552/abd10b`
16. *GNU Octave: Scientific Programming Language*, `https://octave.org/`
17. *Tracker: Copyright (c) 2020 Douglas Brown*, `https://physlets.org/tracker/`
18. OriginLab Corporation, `https://ww.originlab.com/`
19. PHYWE `https://www.leybold-shop.com/physics/physics-equipment/systems/cassy/sensor-boxes-sensors/physics/combination-spoked-wheel-337464.html`
20. PHYWE `https://www.phywe.com/physics/mechanics/dynamics-motion/air-track-complete_9002_9933/`
21. PHYWE `https://www.leybold-shop.com/chemistry/product-catalogue-chemistry-biology/chemistry-student-experiments/molecule-building-kits-for-students/cassy/sensor-cassy-2-524013.html`
22. PHYWE `https://www.leybold-shop.com/physics/physics-equipment/systems/cassy/sensor-boxes-sensors/physics/timer-s-524074.html`
23. PHYWE `https://www.leybold-shop.com/technology/electrical-engineering/telecommunications-technology/radar-sonar-techniques/doppler-radar/multi-core-cable-6-pole-1-5-m-50116.html`
24. PHYWE `https://www.leybold-shop.com/physics/physics-equipment/systems/cassy/sensor-boxes-sensors/physics/combination-light-barrier-337462.html`
25. RADWAG Balances and Scales. `https://radwag.com/es/`